



# Nuclear magnetic resonance study of hydrogen dynamics in Al(BH<sub>4</sub>)<sub>4</sub>-based hypersalts M[Al(BH<sub>4</sub>)<sub>4</sub>] (M = Na, K, Rb, Cs)



O.A. Babanova<sup>a</sup>, R.V. Skoryunov<sup>a</sup>, A.V. Soloninin<sup>a</sup>, I. Dovgaliuk<sup>b, c</sup>, A.V. Skripov<sup>a, \*</sup>, Y. Filinchuk<sup>b</sup>

<sup>a</sup> Institute of Metal Physics, Ural Branch of the Russian Academy of Sciences, Ekaterinburg 620990, Russia

<sup>b</sup> Institute of Condensed Matter and Nanosciences, Université catholique de Louvain, 1348 Louvain-la-Neuve, Belgium

<sup>c</sup> Swiss-Norwegian Beamlines, European Synchrotron Radiation Facility, 38042, Grenoble Cedex 9, France

## ARTICLE INFO

### Article history:

Received 9 August 2017

Received in revised form

1 February 2018

Accepted 15 February 2018

Available online 16 February 2018

### Keywords:

A. Energy storage materials

C. Diffusion

D. Nuclear resonances

## ABSTRACT

In order to study the dynamical properties of the novel series of complex hydrides M[Al(BH<sub>4</sub>)<sub>4</sub>] (M = Na, K, Rb, Cs), we have measured the <sup>1</sup>H and <sup>11</sup>B spin-lattice relaxation rates and the <sup>1</sup>H nuclear magnetic resonance spectra in these compounds over broad temperature ranges (6–384 K) and resonance frequency ranges (14–90 MHz). For all the studied compounds, the behavior of the spin-lattice relaxation rates is governed by the reorientational motion of BH<sub>4</sub> groups. For Na[Al(BH<sub>4</sub>)<sub>4</sub>], the temperature dependences of the measured <sup>1</sup>H and <sup>11</sup>B spin-lattice relaxation rates suggest a coexistence of two reorientational processes with different characteristic jump rates and the activation energies of 186(7) and 262(9) meV. For K[Al(BH<sub>4</sub>)<sub>4</sub>], Rb[Al(BH<sub>4</sub>)<sub>4</sub>], and Cs[Al(BH<sub>4</sub>)<sub>4</sub>], the relaxation data are satisfactorily described by the model with a Gaussian distribution of the activation energies and the average activation energies of 393(6), 360(5), and 353(5) meV, respectively. The barriers for reorientational motion in M[Al(BH<sub>4</sub>)<sub>4</sub>] are discussed on the basis of changes in the local environment of BH<sub>4</sub> groups.

© 2018 Elsevier B.V. All rights reserved.

## 1. Introduction

Metal borohydride complexes and their derivatives are considered as promising hydrogen storage materials due to their high hydrogen content [1]. However, practical use of the alkali and alkaline-earth borohydrides is hindered by their stability with respect to thermal decomposition, which leads to high temperatures of hydrogen release. The desorption temperature can be strongly reduced for bimetallic borohydrides, such as NaZn<sub>2</sub>(BH<sub>4</sub>)<sub>5</sub>, NaZn(BH<sub>4</sub>)<sub>3</sub> [2], KCd(BH<sub>4</sub>)<sub>3</sub>, and K<sub>2</sub>Cd(BH<sub>4</sub>)<sub>4</sub> [3], using the correlation between the Pauling electronegativity of metal cations and the decomposition temperature [4]. Bimetallic borohydrides containing light metal atoms are preferable from the point of view of gravimetric H content. Therefore, Al-containing compounds have attracted much recent attention [5–9]. Aluminum borohydride, Al(BH<sub>4</sub>)<sub>3</sub>, having a gravimetric H density of 16.8 wt %, appears to be unsuitable for hydrogen storage since it is a highly pyrophoric and explosive liquid at room temperature [10]. The series of M

[Al(BH<sub>4</sub>)<sub>4</sub>] compounds (where M is an alkali metal) prepared by the reaction of solid MBH<sub>4</sub> with liquid Al(BH<sub>4</sub>)<sub>3</sub> are not so dangerous while retaining high gravimetric H density (for light M elements) [5–9]. In these compounds, [Al(BH<sub>4</sub>)<sub>4</sub>]<sup>−</sup> plays the role of a complex anion. According to the concept introduced in Refs. [11,12], this complex anion can be referred to as “hyperhalogen” which has the electron affinity much exceeding that of halogen ions. Thus, M[Al(BH<sub>4</sub>)<sub>4</sub>] compounds can be considered as hypersalts. The first compound of this series, K[Al(BH<sub>4</sub>)<sub>4</sub>], was synthesized by Semenko et al. [13] in 1972. The structures and hydrogen-storage properties of M[Al(BH<sub>4</sub>)<sub>4</sub>] compounds (M = Na, K, Rb, Cs) were investigated in Refs. [5–9]. All these compounds contain a distorted tetrahedral complex anion [Al(BH<sub>4</sub>)<sub>4</sub>]<sup>−</sup> where BH<sub>4</sub> groups are coordinated to the central aluminum via edges. The room-temperature crystal structure of Na[Al(BH<sub>4</sub>)<sub>4</sub>] is monoclinic (space group C2/c); this compound decomposes at about 363 K. Both K[Al(BH<sub>4</sub>)<sub>4</sub>] and Rb[Al(BH<sub>4</sub>)<sub>4</sub>] have the orthorhombic structure (space group Fddd), and their decomposition temperatures are near 433 K. Upon heating, Cs[Al(BH<sub>4</sub>)<sub>4</sub>] transforms from the low-T phase to the high-T phase near 358 K. The structure of the low-T phase is not yet resolved, and the high-T phase is tetragonal (space group I4<sub>1</sub>/amd); this phase starts to decompose near 423 K.

\* Corresponding author.

E-mail address: [skripov@imp.uran.ru](mailto:skripov@imp.uran.ru) (A.V. Skripov).

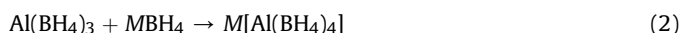
Since  $\text{BH}_4$  groups in borohydrides are known to exhibit fast reorientational motion [14–18], their dynamical behavior is expected to contribute strongly to the balance of energies determining the stability of these materials. The dynamical properties of  $[\text{Al}(\text{BH}_4)_4]^-$  anions have not been studied so far. In the present work, we investigate the dynamical behavior of complex anions in the series of  $M[\text{Al}(\text{BH}_4)_4]$  compounds ( $M = \text{Na}, \text{K}, \text{Rb}, \text{Cs}$ ) using nuclear magnetic resonance (NMR) measurements of the  $^1\text{H}$  and  $^{11}\text{B}$  spin-lattice relaxation rates and the  $^1\text{H}$  spectra over wide temperature and resonance frequency ranges.

## 2. Experimental details

The synthesis of the bimetallic borohydrides  $M[\text{Al}(\text{BH}_4)_4]$  ( $M = \text{Na}, \text{K}, \text{Rb}, \text{Cs}$ ) was analogous to that described in Refs. [6,7,9]. All reactions were performed using the commercially available materials:  $\text{AlCl}_3$ ,  $\text{LiBH}_4$ ,  $\text{NaBH}_4$ ,  $\text{KBH}_4$  (Sigma-Aldrich),  $\text{RbBH}_4$  and  $\text{CsBH}_4$  (Katchem). At the first stage,  $\text{Al}(\text{BH}_4)_3$  was prepared according to the reaction



Since  $\text{Al}(\text{BH}_4)_3$  is highly pyrophoric and explosive in contact with moisture and air, all manipulations were carried out in the dry nitrogen-filled glove-box. At the second stage of synthesis, 1–4 mL of freshly prepared  $\text{Al}(\text{BH}_4)_3$  was transferred via syringe to a flask containing ground powder of  $\text{MBH}_4$  with continuous stirring. The reaction



occurred during 4–7 days. The excess of volatile  $\text{Al}(\text{BH}_4)_3$  was removed by pumping with an oil pump for a few minutes. According to the X-ray powder diffraction (XRPD) analysis, the first cycle of soaking of  $M[\text{Al}(\text{BH}_4)_4]$  in  $\text{Al}(\text{BH}_4)_3$  resulted in the mixture of  $M[\text{Al}(\text{BH}_4)_4]$  and  $\text{MBH}_4$  with a nearly 1:1 weight ratio. After the second cycle of soaking the well-ground mixture of  $M[\text{Al}(\text{BH}_4)_4]$  and  $\text{MBH}_4$  in  $\text{Al}(\text{BH}_4)_3$ , the yield of the target product in the reaction (2) was about 90 wt %. The structures and the lattice parameters of the dominant  $M[\text{Al}(\text{BH}_4)_4]$  phases derived from the synchrotron powder diffraction data are listed below.  $\text{Na}[\text{Al}(\text{BH}_4)_4]$ :  $C2/c$ ,  $a = 9.3375(3)$  Å,  $b = 11.2499(4)$  Å,  $c = 8.411$  Å,  $\beta = 104.706(2)^\circ$ .  $\text{K}[\text{Al}(\text{BH}_4)_4]$ :  $Fddd$ ,  $a = 9.7405(3)$  Å,  $b = 12.4500(4)$  Å,  $c = 14.6975(4)$  Å.  $\text{Rb}[\text{Al}(\text{BH}_4)_4]$ :  $Fddd$ ,  $a = 9.8889(4)$  Å,  $b = 13.3009(7)$  Å,  $c = 14.3252(8)$  Å.  $\text{Cs}[\text{Al}(\text{BH}_4)_4]$  (high- $T$  phase):  $I4_1/amd$ ,  $a = 7.8594(3)$  Å,  $c = 16.3173(8)$  Å. For NMR experiments, the powdered samples were flame-sealed in glass tubes under  $\sim 0.5$  bar of nitrogen gas.

NMR measurements were performed on a pulse spectrometer with quadrature phase detection at the frequencies  $\omega/2\pi = 14, 28$  and  $90$  MHz for  $^1\text{H}$  and  $28$  MHz for  $^{11}\text{B}$ . In order to avoid slow changes in the sample composition [7], for each of the samples the upper limits of the temperature range of NMR measurements were about 40–50 K lower than the actual decomposition temperatures. The magnetic field was provided by a 2.1 T iron-core Bruker magnet. A home-built multinuclear continuous-wave NMR magnetometer working in the range 0.32–2.15 T was used for field stabilization. For rf pulse generation, we used a home-built computer-controlled pulse programmer, a PTS frequency synthesizer (Programmed Test Sources, Inc.) and a 1 kW Kalmus wideband pulse amplifier. Typical values of the  $\pi/2$  pulse length were 2–3  $\mu\text{s}$  for both  $^1\text{H}$  and  $^{11}\text{B}$ . A probehead with the sample was placed into an Oxford Instruments CF1200 continuous-flow cryostat using nitrogen or helium as a cooling agent. The sample temperature monitored by a chromel – (Au-Fe) thermocouple was stable to

$\pm 0.1$  K. The nuclear spin-lattice relaxation rates were measured using the saturation – recovery method. NMR spectra were recorded by Fourier transforming the solid echo signals (pulse sequence  $\pi/2_x - t - \pi/2_y$ ).

## 3. Results and discussion

### 3.1. $\text{Na}[\text{Al}(\text{BH}_4)_4]$ : $^1\text{H}$ and $^{11}\text{B}$ spin-lattice relaxation rates

The behavior of the proton spin-lattice relaxation rates  $R_1^H$  measured at three resonance frequencies for  $\text{Na}[\text{Al}(\text{BH}_4)_4]$  is shown in Fig. 1. It should be noted that the recovery of  $^1\text{H}$  spin magnetization is well described by a single exponential function above 190 K; however, below this temperature, considerable deviations from the single-exponential recovery have been found. The analysis of the data at  $T < 190$  K has shown that the recovery of  $^1\text{H}$  spin magnetization in this range can be satisfactorily approximated by a sum of two exponential components. The points shown in Fig. 1 at  $T < 190$  K correspond to the slower relaxation component which has the dominant amplitude. The behavior of the faster (minor) relaxation component with the rate  $R_{1f}^H$  is shown in Fig. 2. It can be seen that  $R_{1f}^H$  exhibits a maximum near 135 K. Included in Fig. 2 are also the proton spin-lattice relaxation rate data for  $\text{NaBH}_4$  from our previous work [19]. Comparison of the two data sets suggests that the faster relaxation component for our  $\text{Na}[\text{Al}(\text{BH}_4)_4]$  sample can be attributed to the residual  $\text{NaBH}_4$  phase (see the Experimental details section). The relative amplitudes of the faster component are also in reasonable agreement with the fraction of the residual phase derived from X-ray diffraction measurements. Note that near 190 K the sodium borohydride undergoes the first-order transition from the ordered tetragonal phase to the disordered cubic phase, and this transition is accompanied [19] by the sharp drop of  $R_1^H$  (see Fig. 2). Because of this feature, the effects of the residual  $\text{NaBH}_4$  phase on the measured proton relaxation rates become negligible above 190 K. Generally, a contribution of the minor phase to the

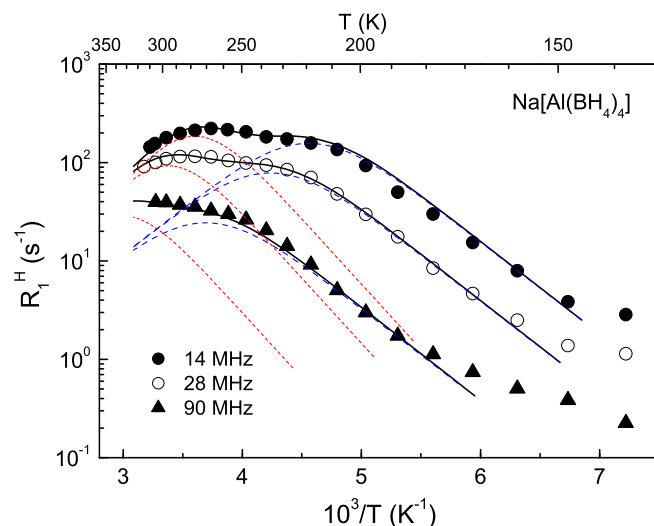


**Fig. 1.** Proton spin-lattice relaxation rates measured at the resonance frequencies  $\omega/2\pi = 14, 28$  and  $90$  MHz for  $\text{Na}[\text{Al}(\text{BH}_4)_4]$  as functions of the inverse temperature. Above 190 K the data points represent the single-exponential approximation of the nuclear magnetization recovery, and below 190 K they correspond to the slower component of the two-exponential recovery. The solid lines show the simultaneous fits of the two-peak model the data. The blue and red dashed lines represent the low- $T$  and high- $T$  peaks, respectively. (For interpretation of the references to colour in this figure legend, the reader is referred to the Web version of this article.)

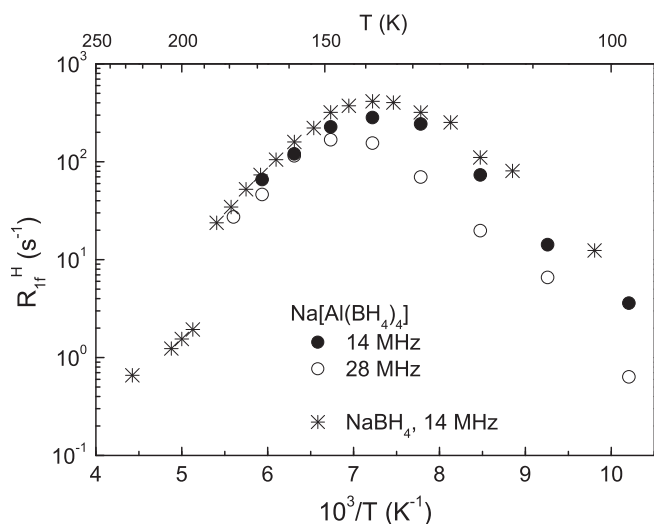


**Fig. 2.** The fast components of the two-exponential proton spin-lattice relaxation at 14 and 28 MHz for  $\text{Na}[\text{Al}(\text{BH}_4)_4]$  as functions of the inverse temperature. The behavior of the proton spin-lattice relaxation rate for  $\text{NaBH}_4$  at 14 MHz [19] is shown for comparison.

total recovery of nuclear magnetization becomes detectable only in the  $T$  range where the corresponding relaxation rate is faster (or of the same order of magnitude) than the relaxation rate for the major phase. In the temperature range where the relaxation rate for the minor phase is much slower than that for the major phase, it is practically impossible to detect a contribution of the minor phase. Thus, for the pure  $\text{Na}[\text{Al}(\text{BH}_4)_4]$  compound, the behavior of the proton relaxation rate should be determined by the experimental  $R_1^H$  data at  $T > 190$  K and by the slower relaxation component below this temperature.

The proton spin-lattice relaxation rate in borohydride-based materials usually shows a peak at the temperature at which the reorientational jump rate  $\tau^{-1}$  of the  $\text{BH}_4$  groups becomes nearly equal to the nuclear magnetic resonance frequency  $\omega$  [15,17]. However, the temperature dependence of  $R_1^H$  for  $\text{Na}[\text{Al}(\text{BH}_4)_4]$  looks like a superposition of two overlapping peaks (Fig. 1). This indicates a coexistence of at least two reorientational processes with different characteristic jump rates [20,21]. Such a coexistence is typical of a linear coordination of each  $\text{BH}_4$  group by two nearest-neighbor metal atoms [21]. Fig. 3 shows the complex  $[\text{Al}(\text{BH}_4)_4]^-$  anion and two types of the coordination environment of  $\text{BH}_4$  groups in  $M[\text{Al}(\text{BH}_4)_4]$  compounds. In  $\text{Na}[\text{Al}(\text{BH}_4)_4]$ , the coordination of all  $\text{BH}_4$  groups is close to the linear one (shown in Fig. 3b), although the actual  $\text{Al} - \text{B} - \text{Na}$  angles deviate from the ideal  $180^\circ$  values [7,9]. As discussed in Ref. [21], the 2-fold symmetry axis parallel to the  $\text{Al} - \text{B} - \text{M}$  line should represent the “easy” axis corresponding to the lowest energy barriers for  $\text{BH}_4$  reorientations and to the fastest motion. Reorientations around two other 2-fold axes (perpendicular to the  $\text{Al} - \text{B} - \text{M}$  line) and/or 3-fold axes should correspond to higher energy barriers and to slower motion. We assume that for each of the two reorientational processes, the temperature dependence of H jump rate  $\tau_i^{-1}$  ( $i = 1$  or  $2$ ) is governed by the Arrhenius law with the activation energy  $E_{ai}$ ,

$$\tau_i^{-1} = \tau_{0i}^{-1} \exp(-E_{ai}/k_B T), \quad (3)$$

and  $i = 1$  corresponds to the faster process responsible for the low-temperature  $R_1^H(T)$  peak. In our two-peak model, the resulting proton spin-lattice relaxation rate is expressed as

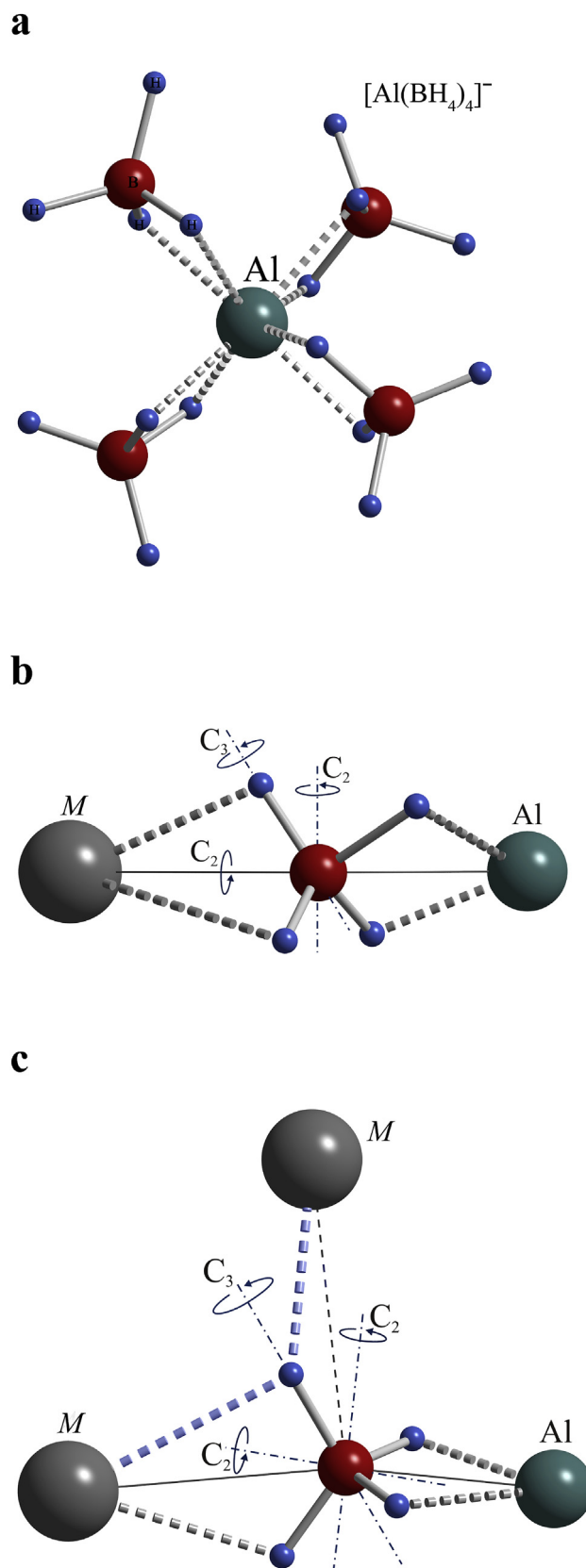


**Fig. 3.** Schematic views of the complex  $[\text{Al}(\text{BH}_4)_4]^-$  anion (a), the linear (b) and the triangular (c) coordination of  $\text{BH}_4$  groups in  $M[\text{Al}(\text{BH}_4)_4]$  compounds.

$$R_1^H = \sum_{i=1}^2 R_{1i}^H, \quad (4)$$

where the contributions  $R_{1i}^H$  are related to the corresponding jump rates  $\tau_i^{-1}$  by the standard theory [22] of relaxation due to motionally-modulated dipole-dipole interactions between nuclear spins. In order to understand, what interactions are important for the  $^1\text{H}$  spin-lattice relaxation in our system, we have calculated the 'rigid-lattice' second moments for the  $^1\text{H} - ^1\text{H}$ ,  $^1\text{H} - ^{11}\text{B}$ ,  $^1\text{H} - ^{27}\text{Al}$ , and  $^1\text{H} - ^{23}\text{Na}$  dipole-dipole interactions on the basis of the structural data [7,9] for  $\text{Na}[\text{Al}(\text{BH}_4)_4]$ :  $M_{2\text{HH}} = 1.84 \times 10^{10} \text{ s}^{-2}$ ,  $M_{2\text{HB}} = 1.43 \times 10^{10} \text{ s}^{-2}$ ,  $M_{2\text{HAl}} = 9.41 \times 10^9 \text{ s}^{-2}$ , and  $M_{2\text{HNa}} = 8.75 \times 10^8 \text{ s}^{-2}$ . These results show that the H – H, H – B, and H – Al interactions are of comparable strength, while the H – Na interactions are much weaker and can be neglected. Therefore, the expression for  $R_{1i}^H$  can be written in the form:

$$R_{1i}^H = \frac{2\Delta M_{\text{HH}}\tau_{ci}}{3} \left[ \frac{1}{1 + \omega_{\text{H}}^2\tau_{ci}^2} + \frac{4}{1 + 4\omega_{\text{H}}^2\tau_{ci}^2} \right] + \frac{\Delta M_{\text{HB}}\tau_{ci}}{2} \left[ \frac{1}{1 + (\omega_{\text{H}} - \omega_{\text{B}})^2\tau_{ci}^2} + \frac{3}{1 + \omega_{\text{H}}^2\tau_{ci}^2} + \frac{6}{1 + (\omega_{\text{H}} + \omega_{\text{B}})^2\tau_{ci}^2} \right] + \frac{\Delta M_{\text{HAl}}\tau_{ci}}{2} \left[ \frac{1}{1 + (\omega_{\text{H}} - \omega_{\text{Al}})^2\tau_{ci}^2} + \frac{3}{1 + \omega_{\text{H}}^2\tau_{ci}^2} + \frac{6}{1 + (\omega_{\text{H}} + \omega_{\text{Al}})^2\tau_{ci}^2} \right] \quad (5)$$

where  $\omega_{\text{H}}$ ,  $\omega_{\text{B}}$ , and  $\omega_{\text{Al}}$  are the resonance frequencies of  $^1\text{H}$ ,  $^{11}\text{B}$ , and  $^{27}\text{Al}$ , respectively, and  $\Delta M_{\text{HHi}}$ ,  $\Delta M_{\text{HBi}}$ , and  $\Delta M_{\text{HAli}}$  are the parts of the dipolar second moments due to H – H, H – B, and H – Al interactions that are caused to fluctuate by the  $i$ th reorientational process. The dipolar correlation times  $\tau_{ci}$  are simply related to the corresponding mean residence times  $\tau_i$  between successive H jumps:  $\tau_{ci} = \tau_i$  for H – B, H – Al interactions and H – H interactions within the same  $\text{BH}_4$  group, and  $\tau_{ci} = \tau_i/2$  for H – H interactions between different  $\text{BH}_4$  groups. Since each of the H – H, H – B, and H – Al terms in Eq. (5) exhibits nearly the same temperature and frequency dependence, it is practically impossible to determine the amplitude factors  $\Delta M_{\text{HHi}}$ ,  $\Delta M_{\text{HBi}}$ , and  $\Delta M_{\text{HAli}}$  independently from the fits to the experimental relaxation rate data. Therefore, we have assumed that the ratios  $\Delta M_{\text{HBi}}/\Delta M_{\text{HHi}}$  and  $\Delta M_{\text{HAli}}/\Delta M_{\text{HHi}}$  are the same as the corresponding calculated 'rigid-lattice' second moment ratios  $M_{2\text{HB}}/M_{2\text{HH}} = 0.78$  and  $M_{2\text{HAl}}/M_{2\text{HH}} = 0.51$  (see above). Thus, the parameters of our two-peak model include the activation energies  $E_{ai}$ , the pre-exponential factors  $\tau_{0i}$ , and the amplitude factors  $\Delta M_{\text{HHi}}$  ( $i = 1, 2$ ). These parameters have been varied to find the best fit of the  $R_1^H(T)$  dependences calculated on the basis of Eqs. (3)–(5) to the experimental data at the three resonance frequencies *simultaneously*. The simultaneous fit procedure means that we look for a single set of parameters minimizing the complex merit function [23] that measures the agreement between the model and the data at all the available resonance frequencies. In our case, the minimization has been done by the nonlinear least squares method using the Levenberg-Marquardt algorithm [23]. The results of this simultaneous fit to the data in the range of 148–315 K are shown by solid curves in Fig. 1. The corresponding motional parameters are  $\tau_{01} = 6.0(5) \times 10^{-13} \text{ s}$ ,  $E_{a1} = 186(7) \text{ meV}$  (for the faster

reorientational process), and  $\tau_{02} = 1.9(2) \times 10^{-13} \text{ s}$ ,  $E_{a2} = 262(9) \text{ meV}$  (for the slower process); the amplitude parameters are  $\Delta M_{\text{HH1}} = 3.63(8) \times 10^9 \text{ s}^{-2}$  and  $\Delta M_{\text{HH2}} = 4.32(7) \times 10^9 \text{ s}^{-2}$ . It should be noted that, for both jump processes, the activation energies are in the range of typical  $E_a$  values for  $\text{BH}_4$  reorientations in borohydrides [15,17]. The values of  $\Delta M_{\text{HH1}}$  and  $\Delta M_{\text{HH2}}$  are considerably smaller than the calculated 'rigid-lattice' second moment  $M_{2\text{HH}}$ ; this feature reflects the fact that *localized* H motion (such as  $\text{BH}_4$  reorientations) averages only a part of H – H dipolar interactions in the system. We shall return to this point below, in the course of discussion of the  $^1\text{H}$  NMR line widths. It should also be noted that at low temperatures the measured  $R_1^H$  values tend to level off (see Fig. 1). This feature may indicate the presence of additional relaxation mechanisms (such as due to spin diffusion to paramagnetic impurities) that become relatively more important at low temperatures. Similar contributions were found in a number of complex borohydrides, for example, in  $\text{LiZn}_2(\text{BH}_4)_5$  [24].

Although boron atoms do not participate in the reorientational

motion of  $\text{BH}_4$  groups,  $^{11}\text{B}$  NMR measurements can probe the reorientations via the fluctuating  $^{11}\text{B} - ^1\text{H}$  dipole-dipole and quadrupole interactions. The  $^{11}\text{B}$  spin-lattice relaxation in  $\text{Na}[\text{Al}(\text{BH}_4)_4]$  is found to be non-exponential over the entire temperature range studied; however, it can be reasonably approximated by a sum of two exponential functions. The two-exponential recovery of the  $^{11}\text{B}$  nuclear magnetization was previously observed in a number of borohydrides [25–28]. Such a behavior can be attributed [22] to the non-zero electric quadrupole moment of this nucleus. It should be stressed that the nature of deviations from a single-exponential relaxation for  $^{11}\text{B}$  differs from that for  $^1\text{H}$ ; this is consistent with the fact that the  $^{11}\text{B}$  relaxation is two-exponential even in the temperature range ( $T > 190 \text{ K}$ ) where the  $^1\text{H}$  relaxation is single-exponential. The temperature dependence of the fast (dominant) component of the  $^{11}\text{B}$  spin-lattice relaxation rate,  $R_{1f}^B$ , at 28 MHz in the temperature range 188–298 K is shown in Fig. 4. Comparison of Figs. 4 and 1 indicates that general features of the behavior of  $R_{1f}^B$  in  $\text{Na}[\text{Al}(\text{BH}_4)_4]$  are similar to those of the  $^1\text{H}$  spin-lattice relaxation rate, although the scatter of the  $R_{1f}^B$  data is more pronounced than that of the  $R_1^H$  data. The scatter of the  $R_{1f}^B$  data in Fig. 4 may be attributed to a certain instability of the two-exponential description of the recovery curves. The similarity between the  $^{11}\text{B}$  and  $^1\text{H}$  relaxation data suggests that the observed  $R_{1f}^B$  peaks originate from the same types of  $\text{BH}_4$  reorientations as the corresponding  $R_1^H$  peaks. In order to support this conclusion, we have fitted the two-peak model to the  $R_{1f}^B(T)$  data, using the motional parameters found from the  $R_1^H(T)$  fit as the starting set of parameters. The fitting procedure demonstrates a fast convergence,

and the results are shown in Fig. 4. The corresponding motional parameters are  $\tau_{01} = 9.3(6) \times 10^{-13}$  s,  $E_{a1} = 182(7)$  meV (for the faster process), and  $\tau_{02} = 1.1(2) \times 10^{-13}$  s,  $E_{a2} = 274(8)$  meV (for the slower process). Thus, the  $^{11}\text{B}$  spin-lattice relaxation data for Na  $[\text{Al}(\text{BH}_4)_4]$  can be satisfactorily described by the set of motional parameters which are very close to those derived from the  $^1\text{H}$  relaxation results.

### 3.2. $\text{K}[\text{Al}(\text{BH}_4)_4]$ , $\text{Rb}[\text{Al}(\text{BH}_4)_4]$ , and $\text{Cs}[\text{Al}(\text{BH}_4)_4]$ : $^1\text{H}$ and $^{11}\text{B}$ spin-lattice relaxation rates

General features of the behavior of the proton spin-lattice relaxation rates in  $\text{K}[\text{Al}(\text{BH}_4)_4]$ ,  $\text{Rb}[\text{Al}(\text{BH}_4)_4]$ , and  $\text{Cs}[\text{Al}(\text{BH}_4)_4]$  are similar. Therefore, we adopt a parallel discussion of the relaxation results for these three compounds. As in the case of  $\text{Na}[\text{Al}(\text{BH}_4)_4]$ , the recovery of the  $^1\text{H}$  nuclear magnetization in these compounds is found to deviate from a single-exponential behavior at low temperatures (below about 240 K, 208 K, and 228 K for  $M = \text{K}$ ,  $\text{Rb}$ , and  $\text{Cs}$ , respectively). In the low- $T$  range, the recovery is satisfactorily described by a sum of two exponential components. The faster (minor) relaxation rate component can be attributed to the residual  $\text{MBH}_4$  phases; this component shows a peak near 130 K, 120 K, and 100 K for  $M = \text{K}$ ,  $\text{Rb}$ , and  $\text{Cs}$ , respectively, as in the corresponding  $\text{MBH}_4$  compounds [19,29]. Thus, the pure  $M[\text{Al}(\text{BH}_4)_4]$  phases should be characterized by the experimental  $R_1^H$  values in the high- $T$  range and by the slower (dominant) relaxation rate component in the low- $T$  range; such relaxation rates for  $\text{K}[\text{Al}(\text{BH}_4)_4]$ ,  $\text{Rb}[\text{Al}(\text{BH}_4)_4]$ , and  $\text{Cs}[\text{Al}(\text{BH}_4)_4]$  as functions of the inverse temperature are shown in Fig. 5. It can be seen that for all compounds  $R_1^H(T)$  exhibits the frequency-dependent peak that is typical of the mechanism of nuclear dipole-dipole interaction modulated by atomic motion [22]. In contrast to the case of  $\text{Na}[\text{Al}(\text{BH}_4)_4]$ , there are no signs of two overlapping relaxation rate peaks.

A closer inspection of the data shown in Fig. 5 indicates that for all compounds the observed frequency dependence of  $R_1^H$  at the low-temperature slope of the peak is weaker than the  $\omega^{-2}$  dependence predicted by the standard theory [22]. This feature is

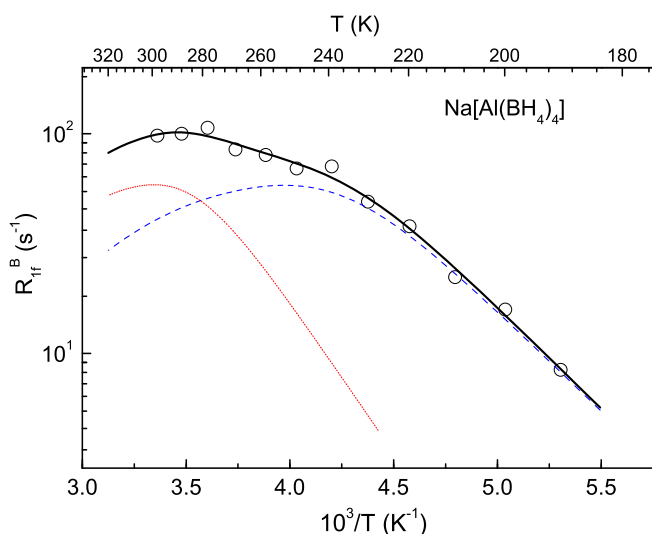
consistent with the presence of a distribution of H jump rates [30]. A certain distribution of the reorientational jump rates in  $\text{K}[\text{Al}(\text{BH}_4)_4]$ ,  $\text{Rb}[\text{Al}(\text{BH}_4)_4]$ , and  $\text{Cs}[\text{Al}(\text{BH}_4)_4]$  may be expected, taking into account the T-shaped triangular coordination of  $\text{BH}_4$  groups in these compounds (see Fig. 3c). In this case, there is no well-defined “easy” reorientational axis, and one may expect more than two rotational processes with different rates. To describe a distribution of H jump rates, we use the simplest model based on a Gaussian distribution of the activation energies [30], where the observed relaxation rate is expressed as

$$R_1^H = \int R_1^H(E_a)G(E_a, \bar{E}_a, \Delta E_a)dE_a. \quad (6)$$

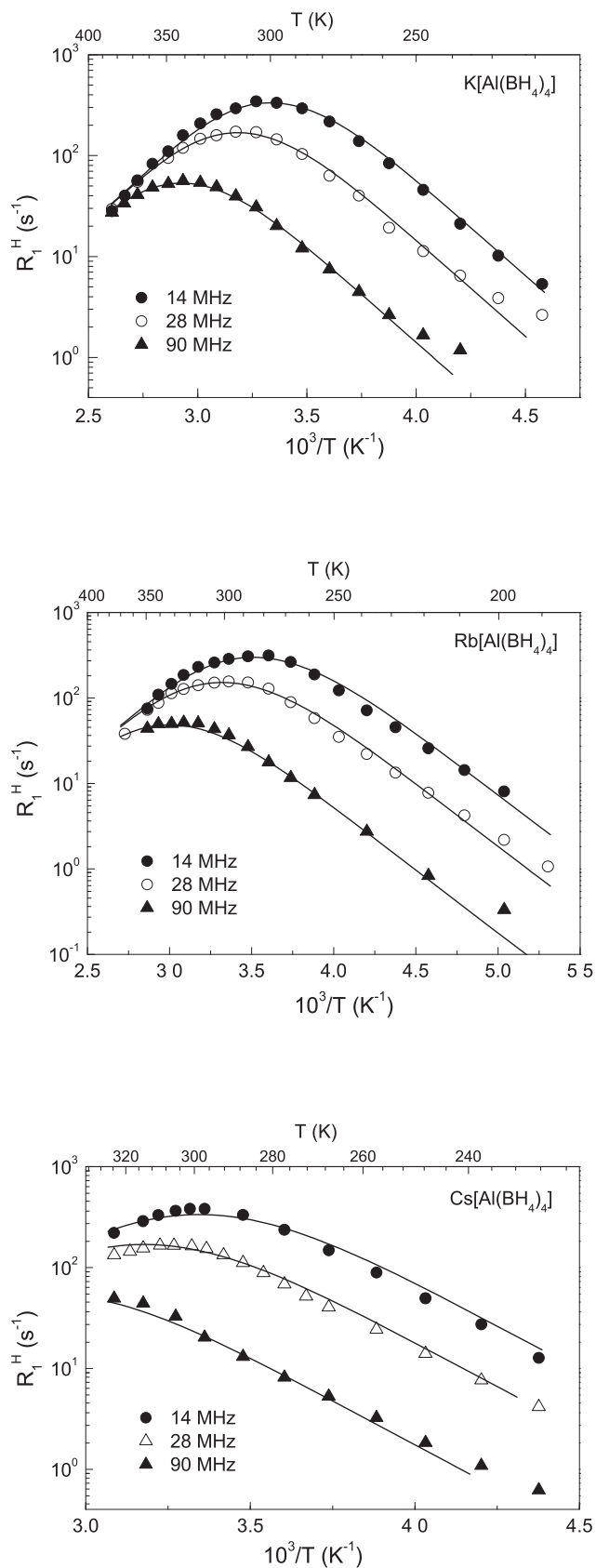
Here  $G(E_a, \bar{E}_a, \Delta E_a)$  is a Gaussian distribution function centered on  $\bar{E}_a$  with the dispersion  $\Delta E_a$ , and  $R_1^H(E_a)$  is determined by combining the standard expression that relates the relaxation rate and  $\tau$  (such as Eq. (5)) and the Arrhenius law (Eq. (3)). The parameters of this model are the average activation energy  $\bar{E}_a$ , the dispersion  $\Delta E_a$ , the pre-exponential factor  $\tau_0$  and the amplitude factor  $\Delta M$  determined by the strength of the fluctuating part of dipole-dipole interaction. As in the case of  $\text{Na}[\text{Al}(\text{BH}_4)_4]$ , we have assumed that the ratios of the fluctuating parts of different interactions,  $\Delta M_{\text{HB}}/\Delta M_{\text{HH}}$  and  $\Delta M_{\text{HAl}}/\Delta M_{\text{HH}}$  are the same as the corresponding calculated ‘rigid-lattice’ second moment ratios  $M_{2\text{HB}}/M_{2\text{HH}}$  and  $M_{2\text{HAl}}/M_{2\text{HH}}$ , on the basis of the structural data [6,7,9]. Since for  $\text{Cs}[\text{Al}(\text{BH}_4)_4]$  the detailed room-temperature structure is still unknown (see above), we have used the structure of the high-temperature phase of this compound [7,9] for the second moment calculations. The motional and amplitude parameters have been varied to find the best fit of the model  $R_1^H(T)$  to the experimental data at three resonance frequencies simultaneously. The results of such simultaneous fits for  $\text{K}[\text{Al}(\text{BH}_4)_4]$ ,  $\text{Rb}[\text{Al}(\text{BH}_4)_4]$ , and  $\text{Cs}[\text{Al}(\text{BH}_4)_4]$  are shown by the solid curves in Fig. 5. The motional parameters resulting from the fits are listed in Table 1. For comparison, the motional parameters of the two reorientational processes in  $\text{Na}[\text{Al}(\text{BH}_4)_4]$  are also included in this table.

As can be seen from Table 1, the lowest values of the activation energies are observed for  $\text{Na}[\text{Al}(\text{BH}_4)_4]$ , while for  $\text{K}[\text{Al}(\text{BH}_4)_4]$ ,  $\text{Rb}[\text{Al}(\text{BH}_4)_4]$ , and  $\text{Cs}[\text{Al}(\text{BH}_4)_4]$  the average activation energies are higher, being close to each other. These results support the notion [31] that the energy barriers for reorientations in borohydrides strongly depend on details of the local environment of  $\text{BH}_4$  groups. The nearly linear coordination of  $\text{BH}_4$  groups by metal atoms appears to be favorable for fast reorientational motion. Another interesting point is the non-monotonic dependence of the activation energy on the cation radius. Note that for cubic alkali-metal borohydrides  $\text{MBH}_4$  ( $M = \text{Na}$ ,  $\text{K}$ ,  $\text{Rb}$ ,  $\text{Cs}$ ), the activation energy for  $\text{BH}_4$  reorientations was also found to change non-monotonically along the series of alkali metals with the maximum for  $M = \text{K}$  [29]. In the case of cubic  $\text{MBH}_4$  compounds, this dependence was rationalized [29] in terms of the ratio  $\delta = (R_M + R_{\text{BH}_4})/d_{M-\text{B}}$  characterizing the deviation of the actual distance  $d_{M-\text{B}}$  between  $M$  ions and  $\text{BH}_4$  groups from the sum of the corresponding ionic radii,  $R_M + R_{\text{BH}_4}$ . A higher value of  $\delta$  indicates a stronger  $M \cdots \text{H}$  interaction, and thus suggests a higher value of the activation energy for  $\text{BH}_4$  reorientations. Indeed, for cubic  $\text{MBH}_4$  borohydrides, the behavior of  $E_a$  was found to be similar to that of  $\delta$  [29]. However, for  $M[\text{Al}(\text{BH}_4)_4]$  compounds, such a simple approach based on geometrical considerations does not work because of more complex structures of these materials and the difference in coordination numbers of different cations.

It should be noted that the thermal stability of  $M[\text{Al}(\text{BH}_4)_4]$  also changes non-monotonically as a function of the cation radius, and the maximum decomposition temperature  $T_{\text{dec}}$  is observed for



**Fig. 4.** The faster component of the  $^{11}\text{B}$  spin-lattice relaxation rate measured at 28 MHz for  $\text{Na}[\text{Al}(\text{BH}_4)_4]$  as a function of the inverse temperature. The solid line shows the fit of the two-peak model to the data. The blue and red dashed lines represent the low- $T$  and high- $T$  peaks, respectively. (For interpretation of the references to colour in this figure legend, the reader is referred to the Web version of this article.)

**Table 1**

Parameters of  $\text{BH}_4$  reorientations resulting from the simultaneous fits to the proton spin-lattice relaxation data in  $\text{Na}[\text{Al}(\text{BH}_4)_4]$ ,  $\text{K}[\text{Al}(\text{BH}_4)_4]$ ,  $\text{Rb}[\text{Al}(\text{BH}_4)_4]$ , and  $\text{Cs}[\text{Al}(\text{BH}_4)_4]$ .

Compound	$E_a$ or $\bar{E}_a$ (meV)	$\Delta E_a$ (meV)	$\tau_0$ (s)	$T$ range (K)
$\text{Na}[\text{Al}(\text{BH}_4)_4]$	186 (7)	–	$6.0 (5) \times 10^{-13}$	148–315
	262 (9)	–	$1.9 (2) \times 10^{-13}$	
$\text{K}[\text{Al}(\text{BH}_4)_4]$	393 (6)	17 (2)	$2.7 (3) \times 10^{-15}$	218–384
$\text{Rb}[\text{Al}(\text{BH}_4)_4]$	360 (5)	30 (4)	$5.3 (3) \times 10^{-15}$	188–367
$\text{Cs}[\text{Al}(\text{BH}_4)_4]$	353 (5)	14 (1)	$1.2 (1) \times 10^{-14}$	228–324

$M = \text{K}$  and  $\text{Rb}$  [7,9]. Furthermore, a certain correlation may be traced between the behavior of the activation energy and that of  $T_{\text{dec}}$ . Fig. 6 shows both  $E_a$  and  $T_{\text{dec}}$  as functions of the cation radius  $R_M$ . For the decomposition temperature, the data include the Li  $[\text{Al}(\text{BH}_4)_4]$  borohydride [7,9]. The values of  $R_M$  are the “effective ionic radii”, as introduced by Shannon [32] for the observed coordination environments [7,9] of  $M$  cations in  $M[\text{Al}(\text{BH}_4)_4]$  by  $\text{BH}_4$  groups (tetrahedral for Li, octahedral for Na, 4+4 for K and Rb, and 4+8 for Cs). It can be seen from Fig. 6 that the behavior of  $E_a$  as a function of the cation radius resembles that of  $T_{\text{dec}}$ . Possible physical grounds for this empirical correlation remain to be elucidated.

As in the case of  $\text{Na}[\text{Al}(\text{BH}_4)_4]$ , the  $^{11}\text{B}$  spin-lattice relaxation in the compounds with  $M = \text{K}$ ,  $\text{Rb}$ , and  $\text{Cs}$  is found to be two-exponential over the entire studied temperature range. For each compound, the faster (dominant) relaxation rate component exhibits a peak in the same temperature range as the corresponding  $^1\text{H}$  relaxation rate peak. Furthermore, the behavior of  $R_{1f}^{B}(T)$  can be satisfactorily described by nearly the same sets of motional parameters as the corresponding  $R_1^H(T)$  data (see Figs. S1 – S3 of the Supporting Information). This means that the behavior of the  $^{11}\text{B}$  spin-lattice relaxation rate is determined by the same reorientational processes, as the proton spin-lattice relaxation rate.

### 3.3. Proton NMR spectra

The main features of the measured  $^1\text{H}$  NMR spectra are similar for all the studied  $M[\text{Al}(\text{BH}_4)_4]$  compounds. As an example of the data, Fig. 7 shows the evolution of the  $^1\text{H}$  NMR spectrum for  $\text{K}[\text{Al}(\text{BH}_4)_4]$  with temperature. At low temperatures, the width  $\Delta\nu$  (full width at half-maximum) of the  $^1\text{H}$  NMR spectrum is determined by dipole-dipole interactions between static nuclear spins; this is the ‘rigid-lattice’ line width  $\Delta\nu_R$ . For  $\text{K}[\text{Al}(\text{BH}_4)_4]$ , the value of

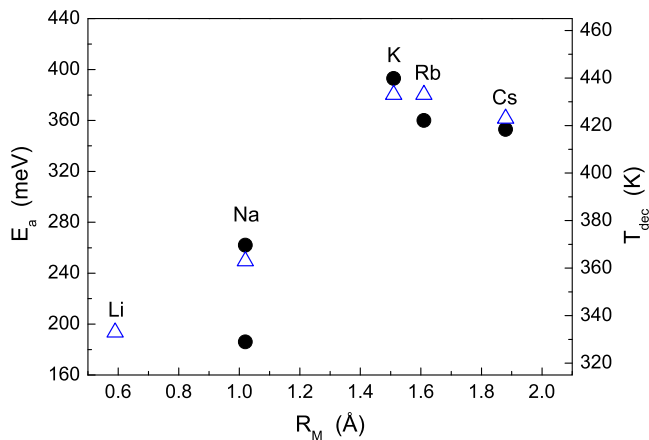


**Fig. 6.** The activation energies for  $\text{BH}_4$  reorientations (solid circles, left-hand scale) and the decomposition temperatures (triangles, right-hand scale) for  $M[\text{Al}(\text{BH}_4)_4]$  as functions of the cation radius.

**Fig. 5.** Proton spin-lattice relaxation rates measured at 14, 28, and 90 MHz for  $\text{K}[\text{Al}(\text{BH}_4)_4]$ ,  $\text{Rb}[\text{Al}(\text{BH}_4)_4]$ , and  $\text{Cs}[\text{Al}(\text{BH}_4)_4]$  as functions of the inverse temperature. The solid lines show the simultaneous fits of the model with a Gaussian distribution of the activation energies to the data.

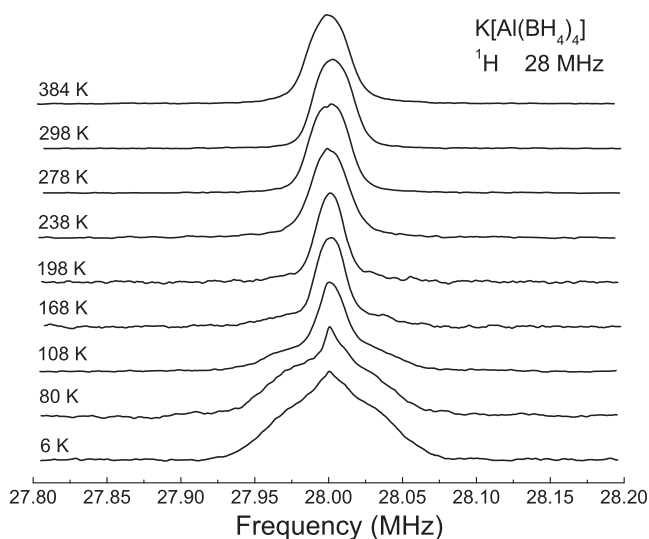


Fig. 7. Evolution of the proton NMR spectrum for  $K[Al(BH_4)_4]$  with temperature.

$\Delta\nu_R$  is about 75 kHz. A rough theoretical estimate of  $\Delta\nu_R$  can be obtained from the second moment calculations using the structural data [7,9]. The calculated ‘rigid lattice’ second moment of the  $^1H$  NMR line for  $K[Al(BH_4)_4]$  is  $4.21 \times 10^{10} s^{-2}$ . Assuming a Gaussian shape of the spectrum, this second moment should correspond to the line width of 77 kHz. Thus, the experimental value of  $\Delta\nu_R$  appears to be close to the estimated one, although the actual shape of the low-temperature spectrum is evidently non-Gaussian (Fig. 7). With increasing temperature,  $\Delta\nu$  starts to decrease due to a partial averaging of dipole-dipole interactions, when the H jump rate  $\tau^{-1}$  becomes nearly equal to  $2\pi\Delta\nu_R$  [22]. For our samples, a motional narrowing becomes significant at the temperature, at which  $\tau^{-1}$  reaches the values of the order of  $5 \times 10^4 s^{-1}$ . It should be noted that for  $BH_4$  reorientations, the line narrowing is not complete, since such a localized H motion leads to only partial averaging of the dipole-dipole interactions even in the limit  $\tau^{-1} \gg 2\pi\Delta\nu_R$ . Thus, at high temperatures the  $^1H$  NMR line width exhibits a plateau, the height of which is determined mostly by ‘intermolecular’ dipole-dipole interactions (between nuclear spins at different  $BH_4$  groups). This behavior of  $\Delta\nu(T)$  is illustrated in Fig. 8 for Na

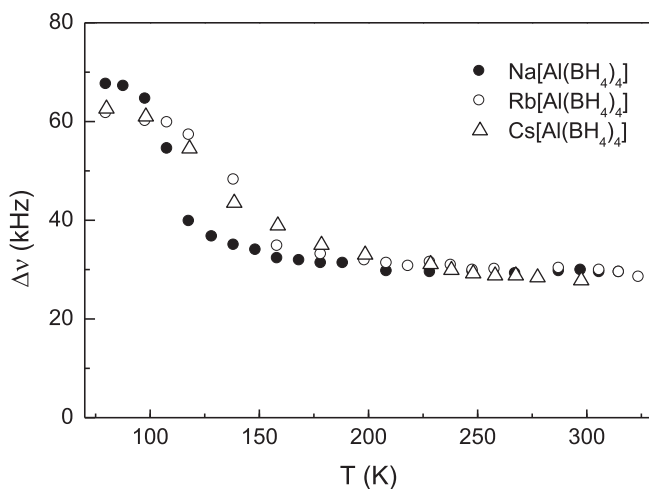


Fig. 8. Temperature dependences of the width (full width at half-maximum) of the  $^1H$  NMR spectra measured for  $Na[Al(BH_4)_4]$ ,  $Rb[Al(BH_4)_4]$ , and  $Cs[Al(BH_4)_4]$  at 28 MHz.

$[Al(BH_4)_4]$ ,  $Rb[Al(BH_4)_4]$ , and  $Cs[Al(BH_4)_4]$ . It should be noted that the characteristic ‘step’ of  $\Delta\nu(T)$  for  $Na[Al(BH_4)_4]$  is observed at lower temperatures than the corresponding ‘steps’ for  $Rb[Al(BH_4)_4]$  and  $Cs[Al(BH_4)_4]$ ; this is consistent with the faster H motion in Na  $[Al(BH_4)_4]$  in the region of the ‘steps’. For all the studied  $M[Al(BH_4)_4]$  compounds, the value of  $\Delta\nu$  at the high-temperature plateau is close to 29 kHz. The expected value of  $\Delta\nu$  at the plateau can be roughly estimated in the following way. Since fast isotropic rotational motion should average out the dipole-dipole interactions within  $BH_4$  groups, we have to calculate only the ‘intermolecular’ contribution to the second moment (between different  $BH_4$  groups and between  $BH_4$  groups and  $^{27}Al$  spins). This contribution can be estimated by placing all the nuclear spins of the group at its center and taking into account only the distances between centers of different groups [33]. The second moment for  $Na[Al(BH_4)_4]$  calculated using this approach is  $3.99 \times 10^9 s^{-2}$ ; for a Gaussian shape of the proton NMR line, this value corresponds to a line width of 23.7 kHz. The experimental value of  $\Delta\nu$  at the plateau is somewhat larger; this may indicate that the actual reorientations are not strictly isotropic.

As can be seen from Fig. 7, the narrowing of the  $^1H$  NMR lines in our systems is not uniform: at intermediate temperatures, the spectra look like superpositions of two components with different widths. This feature is typical of systems with a certain distribution of H jump rates [34], in accordance with the spin-lattice relaxation results for  $M[Al(BH_4)_4]$ . In the range of the high-temperature plateau, the  $^1H$  spectrum looks like a single-component line; this means that the condition  $\tau^{-1} \gg 2\pi\Delta\nu_R$  is fulfilled for all types of reorientational motion.

#### 4. Conclusions

The analysis of the temperature and frequency dependences of the measured proton spin-lattice relaxation rates  $R_1^H$  for the series of bimetallic borohydrides  $M[Al(BH_4)_4]$  ( $M = Na, K, Rb, Cs$ ) has revealed the parameters of reorientational motion of  $BH_4$  groups in these compounds. It is found that for  $Na[Al(BH_4)_4]$  the experimental data are consistent with the coexistence of two reorientational processes having different characteristic jump rates and the activation energies of 186 meV and 262 meV. Such a coexistence is believed to originate from the nearly linear coordination of  $BH_4$  groups by two metal atoms in this compound. For  $K[Al(BH_4)_4]$ ,  $Rb[Al(BH_4)_4]$ , and  $Cs[Al(BH_4)_4]$  compounds with the T-shaped coordination of  $BH_4$  groups, the experimental  $R_1^H$  data are satisfactorily described by the model with a Gaussian distribution of the activation energies and the average activation energies of 393 meV, 360 meV, and 353 meV, respectively. For all the studied compounds, the motional parameters derived from the analysis of the  $^{11}B$  spin-lattice relaxation rates are consistent with those obtained from the proton spin-lattice relaxation data.

#### Acknowledgements

This work was performed within the assignment of the Russian Federal Agency of Scientific Organizations (program ‘Spin’ No. 01201463330). The authors gratefully acknowledge support from the Russian Foundation for Basic Research under Grant No. 16-33-00223 and the Ural Branch of the Russian Academy of Sciences under Grant No. 15-9-2-9.

#### Appendix A. Supplementary data

Supplementary data related to this article can be found at <https://doi.org/10.1016/j.jallcom.2018.02.201>.

## References

- [1] S. Orimo, Y. Nakamori, J.R. Eliseo, A. Züttel, C.M. Jensen, *Chem. Rev.* 107 (2007) 4111–4132.
- [2] D.B. Ravnsbæk, Y. Filinchuk, Y. Cerenius, H.J. Jakobsen, F. Besenbacher, J. Skibsted, T.R. Jensen, *Angew. Chem. Int. Ed.* 48 (2009) 6659–6663.
- [3] D.B. Ravnsbæk, L.H. Sørensen, Y. Filinchuk, F. Besenbacher, T.R. Jensen, *Angew. Chem. Int. Ed.* 51 (2012) 3582–3586.
- [4] Y. Nakamori, K. Miwa, A. Ninomiya, H. Li, N. Ohba, S. Towata, A. Züttel, S. Orimo, *Phys. Rev. B* 74 (2006), 045126.
- [5] D.A. Knight, R. Zidan, R. Lascola, R. Mohtadi, C. Ling, P. Sivasubramanian, J.A. Kaduk, S.-J. Hwang, D. Samanta, P. Jena, *J. Phys. Chem. C* 117 (2013) 19905–19915.
- [6] I. Dovgaliuk, V. Ban, Y. Sadikin, R. Černý, L. Aranda, N. Casati, M. Devillers, Y. Filinchuk, *J. Phys. Chem. C* 118 (2014) 145–153.
- [7] I. Dovgaliuk, PhD Thesis, Université Catholique de Louvain, Louvain-la-Neuve, Belgium, 2015.
- [8] I. Dovgaliuk, Y. Filinchuk, *Int. J. Hydrogen Energy* 41 (2016) 15489–15504.
- [9] I. Dovgaliuk, D.A. Safin, N.A. Tumanov, F. Morelle, A. Moulai, R. Černý, Z. Łodziana, M. Devillers, Y. Filinchuk, *ChemSusChem* 10 (2017) 4725–4734.
- [10] H. Nöth, R. Rurländer, *Inorg. Chem.* 20 (1981) 1062–1072.
- [11] G.L. Gutsev, A.I. Boldyrev, *Chem. Phys.* 56 (1981) 277–283.
- [12] M. Willis, M. Gotz, A.K. Kandalam, G.F. Ganteför, P. Jena, *Angew. Chem. Int. Ed.* 49 (2010) 8966–8970.
- [13] K.N. Semenenko, O.V. Kravchenko, *Russ. J. Inorg. Chem.* 17 (1972) 1084–1086.
- [14] T. Tsang, T.C. Farrar, *J. Chem. Phys.* 50 (1969) 3498–3502.
- [15] A.V. Skripov, A.V. Soloninin, O.A. Babanova, *J. Alloys Compd.* 509S (2011) S535–S539.
- [16] D.T. Shane, L.H. Rayhel, Z. Huang, J.C. Zhao, X. Tang, V. Stavila, M.S. Conradi, *J. Phys. Chem. C* 115 (2011) 3172–3177.
- [17] A.V. Skripov, A.V. Soloninin, O.A. Babanova, R.V. Skoryunov, *J. Alloys Compd.* 645 (2015) S428–S433.
- [18] A. Gradišek, L.H. Jepsen, T.R. Jensen, M.S. Conradi, *J. Phys. Chem. C* 120 (2016) 24646–24654.
- [19] O.A. Babanova, A.V. Soloninin, A.P. Stepanov, A.V. Skripov, Y. Filinchuk, *J. Phys. Chem. C* 114 (2010) 3712–3718.
- [20] A.V. Skripov, A.V. Soloninin, Y. Filinchuk, D. Chernyshov, *J. Phys. Chem. C* 112 (2008) 18701–18705.
- [21] A.V. Skripov, A.V. Soloninin, O.A. Babanova, H. Hagemann, Y. Filinchuk, *J. Phys. Chem. C* 114 (2010) 12370–12374.
- [22] A. Abragam, *The Principles of Nuclear Magnetism*, Clarendon Press, Oxford, 1961.
- [23] W.H. Press, B.P. Flannery, S.A. Teukolsky, W.T. Vetterling, *Numerical Recipes in Pascal: the Art of Scientific Computing*, Cambridge University Press, Cambridge, 1989.
- [24] A. Gradišek, D.B. Ravnsbæk, S. Vrtnik, A. Kocjan, J. Lužnik, T. Apih, T.R. Jensen, A.V. Skripov, J. Dolinšek, *J. Phys. Chem. C* 117 (2013) 21139–21147.
- [25] D.T. Shane, L.H. Rayhel, Z. Huang, J.C. Zhao, X. Tang, V. Stavila, M.S. Conradi, *J. Phys. Chem. C* 115 (2011) 3172–3177.
- [26] A.V. Skripov, A.V. Soloninin, M.B. Ley, T.R. Jensen, Y. Filinchuk, *J. Phys. Chem. C* 117 (2013) 14965–14972.
- [27] V. Ban, A.V. Soloninin, A.V. Skripov, J. Hadermann, A. Abakumov, Y. Filinchuk, *J. Phys. Chem. C* 118 (2014) 23402–23408.
- [28] R.V. Skoryunov, A.V. Soloninin, O.A. Babanova, A.V. Skripov, P. Schouwink, R. Černý, *J. Phys. Chem. C* 119 (2015) 19689–19696.
- [29] O.A. Babanova, A.V. Soloninin, A.V. Skripov, D.B. Ravnsbæk, T.R. Jensen, Y. Filinchuk, *J. Phys. Chem. C* 115 (2011) 10305–10309.
- [30] J.T. Markert, E.J. Cotts, R.M. Cotts, *Phys. Rev. B* 37 (1988) 6446–6452.
- [31] A.V. Soloninin, O.A. Babanova, A.V. Skripov, H. Hagemann, B. Richter, T.R. Jensen, Y. Filinchuk, *J. Phys. Chem. C* 116 (2012) 4913–4920.
- [32] R.D. Shannon, *Acta Cryst.* A32 (1976) 751–767.
- [33] E.G. Sorte, S.B. Emery, E.H. Majzoub, T. Ellis-Caleo, Z.L. Ma, B.A. Hamman, S.E. Hayes, R.C. Bowman, M.S. Conradi, *J. Phys. Chem. C* 118 (2014) 5725–5732.
- [34] R.V. Skoryunov, O.A. Babanova, A.V. Soloninin, A.V. Skripov, N. Verdál, T.J. Udovic, *J. Alloys Compd.* 636 (2015) 293–297.